

Contrasting effects of climate change on the invasion risk and biocontrol potential of the invasive *Iris pseudacorus* L. between Northern and Southern Hemisphere

Minuti, Gianmarco; Coetzee, Julie Angela; Stiers, Iris

Published in:
Biological Control

DOI:
[10.1016/j.biocontrol.2023.105290](https://doi.org/10.1016/j.biocontrol.2023.105290)

Publication date:
2023

License:
CC BY-NC-ND

Document Version:
Accepted author manuscript

[Link to publication](#)

Citation for published version (APA):
Minuti, G., Coetzee, J. A., & Stiers, I. (2023). Contrasting effects of climate change on the invasion risk and biocontrol potential of the invasive *Iris pseudacorus* L. between Northern and Southern Hemisphere. *Biological Control*, 184, [105290]. <https://doi.org/10.1016/j.biocontrol.2023.105290>

Copyright

No part of this publication may be reproduced or transmitted in any form, without the prior written permission of the author(s) or other rights holders to whom publication rights have been transferred, unless permitted by a license attached to the publication (a Creative Commons license or other), or unless exceptions to copyright law apply.

Take down policy

If you believe that this document infringes your copyright or other rights, please contact openaccess@vub.be, with details of the nature of the infringement. We will investigate the claim and if justified, we will take the appropriate steps.

CONTRASTING EFFECT OF CLIMATE CHANGE ON THE INVASION RISK AND BIOCONTROL POTENTIAL OF THE INVASIVE MACROPHYTE *IRIS PSEUDACORUS* L. BETWEEN NORTHERN AND SOUTHERN HEMISPHERE

ABSTRACT

Iris pseudacorus is both a prized ornamental and an invasive aquatic plant that tends to grow dense monospecific stands, displacing the local vegetation and altering the hydrology of freshwater ecosystems. Originally from Europe, this species has historically invaded North America, China and Japan, and more recently spread through Argentina, South Africa and Australasia, where it is now a target for biological control. Field surveys within its native range have led to the selection of three candidate biocontrol agents. Prioritizing the best candidates for different regions constitutes a critical step, which could save significant time and resources before further cost-intensive experimental studies are conducted. Climate change is seldom taken into consideration in the prioritization process. In this regard, climatic suitability can be used to model the potential distributions of weeds and their candidate agents, both in space and time, thus allowing to identify areas at risk of invasion and predict where agents will be able to establish long-term. Accordingly, the objectives of this work were i) to predict *I. pseudacorus* invasions and range shifts in the context of climate change; ii) to identify wetland areas most at risk of invasion under present and future climatic conditions; and iii) to prioritize the best suite of candidate biocontrol agents for different invaded ranges, worldwide. To do so, we modelled the present and future (2040-2060) climatic suitability of *I. pseudacorus* and its candidate agents using the software MaxEnt. Our results highlight a clear distinction between predictions for the Northern and Southern Hemispheres. In North America and eastern Asia, the area climatically suitable for *I. pseudacorus* is expected to increase and shift northwards. As for its biocontrol agents, very low suitability is predicted across these regions, further decreasing under future climatic conditions. On the other hand, climatically suitable areas for the plant in South America, southern Africa and Australasia are predicted, on average, to reduce in response to climate change. A decrease in climatic suitability is also expected for its candidate biocontrol agents which, however, would still maintain a significant range overlap with their host. These results can be used to prioritize areas most at risk of invasion and identify which combination of candidates could potentially provide the best level of control across different invaded ranges.

1. INTRODUCTION

Biological invasions are recognized as a major driver of biodiversity loss and environmental degradation (Pyšek et al., 2020), especially in freshwater ecosystems (Santamaria, 2002). In particular, invasive alien aquatic plants (IAAPs) are considered a major threat to these habitats (Vilá et al., 2009). Yellow flag, *Iris pseudacorus* L. (Iridaceae), is a perennial helophyte native to Europe, North Africa and western Asia. Internationally sold as an ornamental plant, this species has

historically invaded North America, China and Japan, and more recently spread through Argentina, South Africa and Australasia, where it is now a target for biological control (Hill & Coetzee, 2017; McGrannachan and Barton, 2019; Gervazoni et al., 2020). Its dense growth, paired with its ability to adapt to a wide range of environmental conditions, allows it to invade a variety of natural and human-disturbed habitats, displacing native communities and altering the hydrology of freshwater ecosystems (Sutherland, 1990; USDA-APHIS, 2013). So far, three candidate biocontrol agents have been selected (Minuti et al., 2021): the flea beetle *Aphthona nonstriata* Goeze (Coleoptera: Chrysomelidae); the seed weevil *Mononychus punctumalbum* Herbst (Coleoptera: Curculionidae); and the sawfly *Rhadinoceraea micans* Klug (Hymenoptera: Tenthredinidae).

Biological control has been used, with remarkable levels of success, against other aquatic weeds (Hill & Coetzee, 2017; Simberloff, 2021). As such, it holds the potential to be a sustainable solution to the problem, especially when other methods have been ineffective (Hussner et al., 2017). However, the costs and time-frames of developing and implementing biological control are not insignificant. For this reason, prioritizing the best suite of biocontrol agents and identifying areas of release are fundamental steps in order to maximise the return on investment (Mukherjee et al., 2021). A fundamental prerequisite for the effective biological control of an invasive species is the ability of its biocontrol agent(s) to establish and thrive within the invaded range. Matching environmental conditions between native range and release locations increases the chances of survival of the agents and its ability to reproduce, with a direct effect on biological control (Hoelmer & Kirk, 2005). Mismatches are largely, although not solely, driven by climatic factors (Harms et al., 2021). For instance, differences in precipitation and temperature values are reported to affect up to 31% of weed biocontrol programs (Harms et al., 2020). In this context, climate change is expected to significantly influence the distribution of invasive weeds, biocontrol agents, and their interactions (Bellard et al., 2013; Sun et al., 2020; Robinson et al., 2020; Essl et al., 2020). Species distribution models (SDMs) have been increasingly used to identify areas at risk of invasion and, more recently, to prioritize areas for collection and release of biocontrol agents (Mukherjee et al., 2011; Sutton 2019; Minuti et al., 2021). These methods provide useful tools to project the current climatic niche of an organism not only in space but also in time, and can thus be used to analyse climate matching across future climate scenarios (Sun et al., 2017).

Accordingly, the objectives of this work were to use SDMs to i) model *I. pseudacorus* climatic niche and predict its range shifts in response to climate change; ii) identify the most vulnerable wetlands of international importance; and iii) prioritize the best combination of candidates for each invaded range (i.e. North America, Eastern Asia, South America, South Africa and Australasia) based on their current and future climatic suitability.

2. MATERIALS & METHODS

2.1. Occurrence records and variables selection

Worldwide occurrence records for each species were sourced from the Global Biodiversity Information Facility portal (GBIF 2020, 2021). Each dataset was cleaned using the package “*CoordinateCleaner*” (Zizka et al., 2019) in R software 3.6.1 (R Core Development Team, 2019). This allows to remove duplicate records and records assigned to grids centroids, urban areas and biodiversity institutions (i.e. museums, botanical gardens and universities). The datasets were then

visually inspected in QGIS 3.14 (QGIS Development Team, 2020) to identify uncertain records (i.e. geographic outliers, sea-stranded occurrences, doubtful identifications). Uncertain records that could not be confirmed or corrected were excluded from the datasets. Occurrences were then filtered to minimize spatial autocorrelation using the packages ‘*ecospat*’ (Di Cola et al., 2017) and ‘*spThin*’ (Aiello-Lammens et al., 2015). First, in order to avoid pseudo-replication, occurrences were thinned to retain a single record per grid cell (5 arc minutes resolution). Then, a spatial autocorrelation analysis was computed and, based on its results, the data were filtered at distances which minimised the influence of spatial autocorrelation (Boria et al., 2014). This cleaning and filtering method is effective in minimizing the influence of geographic and environmental biases on the data (Sutton, 2019; Minuti et al., 2022). The final datasets consisted of 1140 records for *I. pseudacorus*, 334 records for *A. nonstriata*, 314 records for *M. punctumalbum*, and 180 records for *R. micans* (Supplementary Figure S1).

The predictors used for modelling the present and future climatic suitability of each species were selected from among the bioclimatic variables developed for the BIOCLIM package (Booth et al., 2014), downloaded from WorldClim v2.1. (Fick & Hijmans, 2017). All 19 bioclimatic layers were downloaded at 5 arc minute spatial resolution for historical climate (1970–2020) and for the projected time period 2040–2060. In order to make future projections more reliable, we considered three Global Circulation Models (GCMs) from the most recent version of the World Climate Research Programme Coupled Model Intercomparison Project (WCRP-CMIP6). These were the Model for Interdisciplinary Research on Climate (MIROC6; Shiogama et al., 2019), the Institut Pierre-Simon Laplace Climate Model (IPSL-CM6A-LR; Boucher et al., 2018), and the Hadley Centre Global Environment Model (HadGEM3-GC31-LL; Ridley et al., 2019). These computer-driven mathematical models use current knowledge of dynamical systems paired with predictions of future conditions to accurately simulate the general circulation of planetary atmosphere and oceans in space and time. For each GCM, we considered two Shared Socio-Economic Pathways (SSPs), the ‘middle of the road’ (SSP2 – 4.5) and the ‘fossil-fueled development’ (SSP5 – 8.5) scenarios (Riahi et al., 2017).

After computing pairwise Pearson’s correlation coefficients among predictor variables, a selection was made to minimize multicollinearity (Petitpierre et al., 2016). Amongst highly correlated variables ($|r| > 0.75$), those deemed to hold higher biological relevance for our species, such as temperature extremes and seasonal precipitation values, were retained. The reduced set of variables consisted of: minimum temperature of the coldest month (bio6); mean temperature of the warmest quarter (bio10); annual precipitation (bio12); precipitation seasonality (bio15); and precipitation of the warmest quarter (bio18). The latter has been subject to some criticism due to the presence of discontinuities across its interpolated surface (Escobar et al., 2014). However, such discontinuities are rare on a global scale, and usually limited to the Equatorial regions (Booth, 2022). Upon visual inspection of the layer in QGIS 3.14, no abrupt changes were observed within the areas of interest (i.e. regions already invaded or at risk of invasion by *I. pseudacorus*). Accordingly, the variable was retained for modelling our species. An exception was made for *M. punctumalbum*, for which bio12 and bio18 showed high correlation ($r > 0.75$), and bio18 was therefore excluded. The meaningfulness of these predictors was further assessed by visual inspection of their response curves during model tuning (Supplementary Figure S2).

2.2. Model calibration and evaluation

Climatic suitability models were computed using the software MaxEnt 3.4.1 (Phillips et al., 2017). This program was chosen for its efficiency and numerous applications in presence-background modelling of invasive plant species and biological control agents (Mukherjee et al., 2011; Trethowan et al., 2011; Sutton 2019; Minuti et al., 2022).

After testing optimal model settings using the ‘*SDMtune*’ package (Vignali et al., 2021), MaxEnt settings were set as follows: convergence = 10^5 ; maximum number of iterations = 500; prevalence = 0.5; regularization multiplier = 1; features = lqph. For each model, 10 bootstrap replicates were computed, each randomly allocating 70% of the occurrence records to model training (calibration) and the remaining 30% to model testing (evaluation). The average of all replicates was used for further analyses. Output maps were produced using logistic suitability scores ranging from 0 (low suitability) to 1 (high suitability). Relative contribution of each predictor variable was assessed by their permutation importance (Phillips et al., 2017). After modelling, the Multivariate Environmental Similarity Surface (MESS) was inspected to assess coverage of environmental gradients upon model projection and identify areas of uncertainty (Elith et al., 2010). The respective ‘out-of-range’ environmental variables (i.e. limiting factors) were extrapolated from the dissimilarity maps (MoD) provided by the program output (Elith et al., 2011).

As a first metric of model performance, the area under the receiver operating characteristic curve (AUC) was used. AUC values range from 0.5, identifying models that are no better than random, to 1, indicating excellent model performance (Fielding & Bell, 1997). Model overfitting was evaluated by comparing the average omission rate (OR) of the model with theoretical expectations. OR is the proportion of test localities predicted to fall outside the projected suitable area once the model is converted into a binary prediction by mean of a specific threshold (Boria et al., 2014). Overfit models tend to have higher omission rates than those predicted by the relative threshold, and MaxEnt provides various methods for model thresholding (Merow et al., 2013). In this study, the 10th percentile training presence omission rate (OR10), which sets the threshold at a value that rejects only the lowest 10% of possible predicted occurrences, was used (Boria et al., 2014). Accordingly, models with an OR10 significantly higher than the expected 0.1 were considered overfit (Sutton 2019; Martin et al., 2020). Additionally, as AUC statistic has been subject to some criticism (Lobo et al., 2008), the true presence ratio (TPR) and the Continuous Boyce Index (CBI; mean \pm SD) were employed as additional measures of model accuracy (Hirzel et al., 2006). These threshold-independent metrics are considered more reliable when it comes to validating predictions and transferability of presence-background models (Manzoor et al., 2018). These metrics were calculated using the package ‘*ecospat*’ (Di Cola et al., 2017) in R software 3.6.1.

2.3. Species distribution modelling

The climatic suitability model for *I. pseudacorus* was trained using a combination of native and invaded range occurrences, as this allows the inclusion of the environmental variability acquired by the species in newly colonized areas and produces more reliable approximations than using native or invaded range records alone (Beaumont et al., 2009; Trethowan et al., 2011; Rodriguez-Merino et al., 2019; Martin et al., 2020). Following the method of Hill & Terblanche (2014), background climatic data were drawn from a customized mask generated by selecting Köppen-Geiger climate zones (Beck et al., 2018) containing at least one occurrence record for the species (Minuti et al., 2022). As none

of the candidate biocontrol agents for *I. pseudacorus* is recorded outside of its native European range, only native occurrences were available to use for model training. The distribution of these organisms is less documented, thus, to select a background representative of where the species could potentially occur, a geographic mask of Europe was used (de Jong et al. 2014).

Each model was calibrated using current climatic layers and then projected over the entire world surface. Ten replicates were computed for each future climate projection (MIROC6-SSP2; MIROC6-SSP5; IPSL-SSP2; IPSL-SSP5; HadGEM-SSP2; HadGEM-SSP5), for a total of 60 future models. These were then averaged to produce a single output, expressing suitability in a continuous logistic scale. In order to quantify the geographic area predicted as suitable for each organism, continuous rasters were converted into binary maps by applying the relative OR10 minimum suitability threshold (Sutton, 2019; Martin et al., 2020). In this sense, raster cells with suitability values lower than the OR10 threshold were considered as unsuitable, whereas cells with values higher than the OR10 threshold were considered suitable. Finally, the suitable area for each species across various invaded ranges was calculated using the ‘*raster*’ package (Hijmans, 2017).

2.4. Invasion risk and biocontrol potential

To visualize the effect of climate change on the invasion risk of *I. pseudacorus* worldwide, continuous suitability maps for present and future climatic conditions were overlapped, and difference values extracted for each raster cell, using the *raster calculator* in QGIS. The resulting difference map was then overlapped with an environmental layer containing all wetlands of international importance at a global scale (<https://rsis.ramsar.org/>). Present climatic suitability, future climatic suitability, and difference values were extracted for each Ramsar site using the *point sampling tool* in QGIS. Ramsar sites located within regions climatically unsuitable for *I. pseudacorus* were excluded, whereas the remaining sites were categorized based on their present suitability (Low: 0.3 – 0.5; Medium: 0.5 – 0.7; High: > 0.7) and the prediction for increasing or decreasing climatic suitability under future climatic conditions.

To assess the potential of the candidate biocontrol agents to establish and control *I. pseudacorus* in various regions of interest, binary climatic suitability maps were overlapped in QGIS. Present climatic suitability maps for each candidate biocontrol agent were overlapped with that of *I. pseudacorus* to identify invaded areas where the species could establish and potentially control its target under current climatic conditions. The same procedure was adopted for future suitability maps. Finally, a difference operator was used to calculate the change in climatic suitability and potential climatic niche overlap between present and future projections. All outputs were clipped to the extent of areas currently invaded by *I. pseudacorus* in North America, South America, South Africa, eastern Asia and Australasia. The total area of present and future climatic suitability and niche overlap was calculated for each region of interest using the *raster* package Hijmans, 2017).

3. RESULTS

3.1. Model evaluation and variables contribution

The average AUC values of models trained upon current climate data were 0.710 ± 0.012 for *I. pseudacorus*; 0.898 ± 0.010 for *A. nonstriata*; 0.875 ± 0.014 for *M. punctumalbum*; and 0.956 ± 0.009 for *R. micans* (Table 1). The model discrimination capacity, as measured by its AUC, expresses the

probability that a presence selected at random will have higher predicted suitability than a randomly selected absence (or background). However, a good model is not expected to discriminate beyond the discrimination that the species itself makes in the environment. Therefore, models of generalist species tend to have lower discrimination capacity than those of specialist species (such is the case for *I. pseudacorus*), which does not imply that they are worse models (Sillero et al., 2021). There was no substantial difference between AUC values of present and future climate scenarios, nor across different future climate models, showing agreement among models projected upon different climatic conditions (Table 1). For all models computed, omission rates (OR10) were consistently close to the predicted threshold of 0.1 (indicating no overfitting), true presence ratio (TPR) approached 90%, and CBI values were consistently higher than 0.93, confirming the robustness of model predictions (Table 1). Finally, the Multivariate Environmental Similarity Surface (MESS) showed good coverage of the environmental gradients during model projection, supporting the transferability of our models in time and space (Supplementary Figure S3).

[Table 1 here]

The relative contribution of the climatic variables used as predictors varied slightly between the models for *I. pseudacorus* and its candidate biocontrol agents. Overall, minimum temperature of the coldest month (bio6) was the most influential variable for all four species. For *I. pseudacorus*, this was followed by annual precipitation (bio12), mean temperature of the warmest quarter (bio10) and precipitation of the warmest quarter (bio18), whereas precipitation seasonality (bio15) showed the lowest importance (Table 1). On the other hand, models built for the three candidate biocontrol agents showed little contribution of precipitation-related variables (bio12 and bio18), and were instead highly influenced by temperature-related ones (bio6 and bio10). An exception is observed for precipitation seasonality (bio15), which showed high contribution to models for *A. nonstriata* and *M. punctumalbum*, but little to no contribution to the models built for *R. micans*. Overall, there was no considerable difference in variable contribution to models based on present and future climate scenarios.

3.2. Invasion risk and biocontrol potential

3.2.1. North America

The results of our models predict a northward expansion in the climatically suitable area for *I. pseudacorus* in North America (Fig. 1). Ramsar sites located in southern United States ($n = 25$; 756,502 ha) show a decrease in suitability under future climatic conditions, whereas for those in northern US and Canada ($n = 27$; 347,318 ha), suitability is expected to increase (Fig. 1A). The total area identified as suitable for *I. pseudacorus* will increase by 31.1% (1,515,271 ha) according to our models, with areas of gained suitability in Alaska, northern US and Canada, and regions of lost suitability in south-eastern United States (Fig. 1B). At the same time, areas of climatic suitability for the three candidate biocontrol agents are predicted to decrease (Fig. 1C-E), with *A. nonstriata* and *R. micans* showing little to no suitability across North America, and *M. punctumalbum* losing 43.9% (1,054,086 ha) of its currently suitable area in eastern US and Canada. Accordingly, the overlap between the climatic niche of *I. pseudacorus* and that of its candidate biocontrol agents combined is predicted to decrease from 45.25% (2,494,915 ha) to 20.98% (1,455,821 ha) under future climatic conditions (Fig. 1F).

[Figure 1 here]

3.2.2. Eastern Asia

A similar northward shift in climatic suitability for *I. pseudacorus* is predicted across eastern Asia (Fig. 2). The majority (n = 67; 1,244,394 ha) of Ramsar sites currently at risk of invasion show decreased suitability under future climatic conditions, while the remaining (n = 26; 234,171 ha) show increased suitability (Fig. 2A). Nonetheless, most of the region is expected to remain highly suitable for the weed (Fig. 2B). No suitability is predicted for the flea beetle *A. nonstriata*, both under current and future climate (Fig. 2C). For the weevil *M. punctumalbum*, the limited suitable area currently predicted in northern Japan is expected to be completely lost due to climate change (Fig. 2D). Finally, for the sawfly *R. micans*, currently suitable areas in the Yunnan province of south-western China are predicted to decrease by 37.7% (174,441 ha) in the future (Fig. 2E). Overall, the climatic niche overlap between *I. pseudacorus* and its candidate biocontrol agents is predicted to decrease from 17% (551,783 ha) to 10.5% (353,276 ha) in China and from 37.2% (136,684 ha) to 0.7% (2,590 ha) in Japan (Fig. 2F).

[Figure 2 here]

3.2.3. South America

The predicted climatic suitability for *I. pseudacorus* in South America shows an overall decrease in southern Brazil, Uruguay and north-east Argentina, and an expansion towards the south-western border of Argentina and southern Chile (Fig. 3). Out of the 17 Ramsar sites currently at risk of invasion, 15 (2,138,866 ha) are expected to decrease in suitability in the future, and only 2 (6,257 ha) to increase (Fig. 3A). The total area identified as suitable for the weed is predicted to decrease by 14% (245,352 ha), with only small regions of southern Chile becoming newly suitable to the weed (Fig. 3B). The same pattern is observed for its candidate biocontrol agents. Climatically suitable areas are predicted to decrease by 42.6% (198,494 ha) for *A. nonstriata* (Fig. 3C), by 11% (108,416 ha) for *M. punctumalbum* (Fig. 3D), and by 82.2% (155,691 ha) for *R. micans*, with limited regions of newly acquired suitability in southern Argentina and Chile (Fig. 3E). Despite this decrease, only a minor effect is expected on the overlap between the climatic niche of the weed and that of its candidate biocontrol agents, from 40.8% (716,135 ha) under current climate to 35.1% (533,464 ha) under future climatic conditions (Fig. 3F).

[Figure 3 here]

3.2.4. South Africa

The models predict an overall decrease in climatic suitability for *I. pseudacorus* in southern Africa (Fig. 4). Ramsar sites in the Western Cape, North-West and Limpopo regions (n = 11, 15,210 ha) are expected to decrease in suitability, whereas for those located in the Eastern Cape, Free State, Gauteng, Mpumalanga and Kwa-Zulu Natal regions (n=7, 265,908 ha), the models predict increased suitability (Fig. 4A). A net decrease of 20.9% (152,767 ha) is predicted in the total area suitable for *I. pseudacorus*, with no areas of gained suitability (Fig. 4B). A similar pattern is expected for its candidate biocontrol agents. Suitable areas for *A. nonstriata*, *M. punctumalbum*, and *R. micans* are predicted to decrease by 44.5% (28,796 ha), 16% (36,781 ha) and 43.3% (122,661 ha), respectively (Fig. 4C-E). Nonetheless, the overlap in the climatic niche of the weed and its biocontrol agents shows little change, from 41.7% (314,014 ha) to 35.1% (210,178 ha) under future climatic conditions (Fig. 4F).

[Figure 4 here]

3.2.5. Australasia

A contrasting scenario is predicted for Australasia, with the climatic suitability for *I. pseudacorus* showing a decrease in Australia and an increase, albeit small, in New Zealand (Fig. 5). Accordingly, most Ramsar sites currently at risk of invasion in Australia show decreased suitability ($n = 27$, 610,528 ha), with some exceptions located in south-eastern Australia and Tanzania ($n = 10$, 16,922 ha), for which suitability is predicted to increase (Fig. 3A). In contrast, in New Zealand a decrease is predicted for 3 Ramsar sites (27,858 ha) and an increase for 4 sites (39,328 ha). The total area identified as suitable for the weed is expected to decrease by 28.4% (469,202 ha) in Australia and increase by 1.75% (4,495 ha) in New Zealand (Fig. 5B). The same pattern is predicted for *A. nonstriata* and *M. punctumalbum*, the former showing a 30.6% (107,868 ha) decrease in Australia and a 16.7% (34,320 ha) increase in New Zealand, and the latter a 25.7% (554,839 ha) decrease in Australia and a 27.6% (45,172 ha) increase in New Zealand (Fig. 5C-D). Finally, the suitable area for *R. micans* is predicted to decrease in both ranges, by 55.4% (186,230 ha) in Australia and by 13.3% (20,376 ha) in New Zealand (Fig. 5E). The climatic niche overlap between *I. pseudacorus* and its candidate biocontrol agents is predicted to decrease slightly from 85.9% (1,380,690 ha) to 83.5% (1,008,914 ha) in Australia, and increase from 80.7% (207,449 ha) to 89.9% (230,217 ha) in New Zealand (Fig. 5F).

[Figure 5 here]

4. DISCUSSION

Modelling the environmental suitability of IAAPs can significantly improve the cost-effectiveness of management strategies by directing response efforts towards the most vulnerable areas and helping spread-limitation campaigns (Cordeiro et al., 2020). This holds especially true for weed biological control, where climatic mismatches have been known to affect the outcome of over one-third of reviewed programmes (Harms et al., 2020). The present work is one of the few studies where the bioclimatic niche of the weed and its biocontrol agents have been modelled together (Trethowan et al., 2011; Sun et al., 2017), accounting for the potential effects of climate change (Sun et al., 2020). Our results highlight a clear distinction between invaded regions in the Northern and Southern Hemispheres. In North America and eastern Asia, the area climatically suitable for *I. pseudacorus* is expected to shift northwards, maintaining and even increasing its current extent. This could be attributed to the rise in temperatures expected in the near future, making southernmost regions too dry for the plant and at the same time helping it overcome cold stress limitations in northern regions. On the other hand, climatically suitable areas for the plant in South America, southern Africa and Australasia – with the exception of southern Chile and New Zealand – are predicted to reduce significantly in the future. This range contraction in the Southern Hemisphere has been predicted for other invasive species (e.g. Kriticos et al., 2010) and could be attributed to an increase in heat and dry stresses, excluding the plant from areas currently experiencing a humid temperate climate (Beck et al., 2018). It is important to note that, despite an average decrease worldwide, the predicted suitability for most Ramsar sites is predicted to remain well above the minimum suitability threshold used in this study. Therefore these environments should be considered at risk of invasion by *I. pseudacorus*, at least from a climatic perspective. Paired with other local factors (e.g. habitat, soil type, distance from current invasions, etc.), this information can be used to prioritize wetland areas where management and prevention strategies should be deployed in the near future.

For the three candidate biocontrol agents, our models predict limited to no suitability in North America and eastern Asia, further decreasing under future climatic conditions. This pattern undermines the potential use of these biocontrol agents across invaded regions of the Northern Hemisphere. Such doubts are only reinforced by host-specificity issues linked to the plethora of *Iris* species native to these regions, many of which are cultivated for ornamental use (Cantarelli, 2022). The opposite is true for the Southern Hemisphere, where the decrease in climatic suitability for both *I. pseudacorus* and its candidate biocontrol agents could result in a maintained, or even increased (i.e. Australasia) climatic niche overlap in the future. This is an encouraging outcome for the prospective use of biological control in these regions. However, local differences in predictions are observed. The seed weevil *M. punctumalbum* shows the greatest predicted climatic suitability and overlap with *I. pseudacorus* across all invaded regions, making it a priority candidate according to climatic suitability ranking (Sun et al., 2017). It is followed by the flea beetle *A. nonstriata*, whose climatic suitability and overlap are most relevant within humid temperate climates of South America, coastal South Africa and Australasia. These findings confirm previous studies highlighting the climatic mismatch between *A. nonstriata* and *I. pseudacorus* across the Southern Hemisphere (Minuti et al., 2022). Finally, suitability models of the sawfly *R. micans* predict a limited climatic overlap with its host plant, restricted to specific regions of China and north-eastern South Africa. Naturally, the models obtained are only as good as the data used for training them, and it is impossible to completely exclude the presence of biases in the open-source datasets used (Beck et al., 2014). *Mononychus punctumalbum* is known to have a wide distribution across the western Palearctic region, covering a variety of climate types from northern Spain, throughout central Europe, to drier regions of north-eastern Turkey (Gültekin & Korotyaev, 2012). This adaptation to a wide range of geographical and climatic conditions mirrors our findings and supports the prioritization of this candidate biocontrol agent. On the other hand, to our knowledge, specific literature on the distribution of *A. nonstriata* is lacking. The species is reported as present in most European countries (PESI, 2022a), but the majority of available records belong to humid temperate regions of central and northern Europe (Schmitt & Rönn, 2011; GBIF, 2021). Assuming an under-reporting of the species across other European climate zones, our results would be an underestimation of the potential climatic suitability of *A. nonstriata*, which could therefore perform better than expected across *I. pseudacorus* invaded range. Finally, the sawfly *R. micans* is endemic to central and northern Europe, being reported as absent in most Mediterranean and eastern European countries (PESI, 2022b). This selectivity for highly humid climates could explain the limited suitability predicted by our models. The resulting climatic mismatch between *R. micans* and *I. pseudacorus* suggests that the former should be given low priority as a candidate biocontrol agent, compared with the other species examined (Harms et al., 2021). As observed in other studies (Trethowan et al., 2011; Sun et al., 2017), such a result provides a useful pre-evaluation, cutting the time and costs that would have been related to the pursuit of this agent.

Maximum entropy modelling as a technique requires the user to provide presence records of a species and the raster layers to use as predictors (Phillips et al., 2017). The models presented in this study employ only climatic predictors, as the objectives were to identify climatic mismatches between species and observe the effect of climate change on their suitability. As such, this models identify regions of similar climatic conditions to where the studies species are known to occur at the present time, and should not be interpreted as predicting actual limits to their potential distribution (Pearson et al., 2007). The accuracy of these models can be further improved by adding

environmental and anthropic layers as explanatory variables (Cordeiro et al., 2020). Alternatively, mechanistic models can be built using information about the species functional traits and physiological tolerances to environmental conditions (Kearney & Porter, 2009). Combining correlative and mechanistic models of species distribution can be used to refine predictions and provide independent evidences for the effect of climate change (Kearney et al., 2010).

The success of a biocontrol program is linked with the ability of biocontrol agents not only to survive but also to naturally disperse from the introduction site to new invasions (Perez de la O et al., 2020). Our models show high connectivity among climatically suitable regions in the invaded range, especially across the Southern Hemisphere. This provides a great opportunity to prioritize release sites with optimal environmental conditions for agent survival, reproduction, and dispersal (Robertson et al., 2008). We acknowledge that local biotic and abiotic environmental factors will also play an important role in the ability of a candidate to effectively establish and control its host plant. Further research is needed to shed light on specific conditions that might favor or hinder these organisms, in order to improve the selection of release sites. The models presented here constitute a cost-effective pre-evaluation of the invasion potential of the weed and the biocontrol potential of its candidate agents. As such, they will serve as a useful tool for planning both large-scale and local management strategies, as well as reducing the time and costs of conducting further experimental studies on less-than-optimal candidates.

CONCLUSIONS AND RECOMMENDATIONS

The present study produced climatic suitability models of the wetland invader *I. pseudacorus* and its three candidate biocontrol agents on a global scale. These can be used to identify areas at risk of invasion, to direct sampling and management efforts, as well as to avoid climate mismatches when planning biocontrol releases. Furthermore, by integrating current and future climatic scenarios, these models allow to predict the effect of climate change on the potential distribution and climatic niche overlap of these four species. The results highlight a contrasting effect of climate change on the climatic suitability of *I. pseudacorus* and its candidate biocontrol agents between Northern and Southern Hemisphere. Regions of North America and eastern Asia are predicted to become increasingly suitable for *I. pseudacorus*, especially at higher latitudes, with little to no overlap with its candidate biocontrol agents. On the other hand, climatic suitability for the weed is predicted to decrease across the Southern Hemisphere, and as a result the potential overlap with its biocontrol agents will remain stable or even expand (i.e. Australasia). From a methodological perspective, this work constitutes one of the few examples where the climatic suitability of an invasive species and its candidate biocontrol agents have been modelled together, accounting for climate change. This methodology makes use of open-source datasets and does not require high computational power, and should therefore be considered as a first step when evaluating the climatic suitability of other invasive species targeted by biological control.

ACKNOWLEDGEMENTS

The PhD project of G.M. is funded by a strategic basic research fellowship of the Research Foundation - Flanders (FWO SB71). We thank the Vrije Universiteit Brussel (BAS 53 and BAS 42) and the Centre for Biological Control (Rhodes University) for logistic support. *Iris pseudacorus* biological control research in South Africa is funded through the Department of Environmental Affairs, Natural

Resource Management Programmes (previously the Working for Water Programme). The South African Research Chairs Initiative of the Department of Science and Technology and the National Research Foundation of South Africa provided additional funding. Any opinion, finding, conclusion or recommendation expressed in this material is that of the authors, and the National Research Foundation does not accept any liability in this regard.

REFERENCES

- Aiello-Lammens, M.E., Boria, R.A., Radosavljevic, A., Vilela, B., Anderson, R.P., 2015. spThin: an R package for spatial thinning of species occurrence records for use in ecological niche models. *Ecography* 38 (5), 541–545. <https://doi.org/10.1111/ecog.01132>.
- Beaumont, L.J., Gallagher, R.V., Thuiller, W., Downey, P.O., Leishman, M.R., Hughes, L., 2009. Different climatic envelopes among invasive populations may lead to underestimations of current and future biological invasions. *Divers. Distrib.* 15 (3), 409–420. <https://doi.org/10.1111/j.1472-4642.2008.00547.x>.
- Beck, H.E., Zimmermann, N.E., McVicar, T.R., Vergopolan, N., Berg, A., Wood, E.F., 2018. Present and future Köppen-Geiger climate classification maps at 1-km resolution. *Sci. Data* 5 (1), 1–12. <https://doi.org/10.1038/sdata.2018.214>.
- Beck, J., Böller, M., Erhardt, A., Schwanghart, W., 2014. Spatial bias in the GBIF database and its effect on modeling species' geographic distributions. *Ecol. Inf.* 19, 10–15. <https://doi.org/10.1016/j.ecoinf.2013.11.002>.
- Bellard, C., Thuiller, W., Leroy, B., Genovesi, P., Bakkenes, M., Courchamp, F., 2013. Will climate change promote future invasions? *Glob. Change Biol.* 19 (12), 3740–3748. doi: 10.1111/gcb.12344
- Booth, T. H., Nix, H. A., Busby, J. R., Hutchinson, M.F., 2014. BIOCLIM: the first species distribution modelling package, its early applications and relevance to most current MAXENT studies. *Divers. Distrib.* 20 (1), 1-9. doi: 10.1111/ddi.12144
- Booth, T.H., 2022. Checking bioclimatic variables that combine temperature and precipitation data before their use in species distribution models. *Austral Ecology*, 47(7), 1506-1514. doi: 10.1111/aec.13234
- Boria, R.A., Olson, L.E., Goodman, S.M., Anderson, R.P., 2014. Spatial filtering to reduce sampling bias can improve the performance of ecological niche models. *Ecol. Model.* 275, 73–77. <https://doi.org/10.1016/j.ecolmodel.2013.12.012>.
- Boucher, O., Denvil, S., Levavasseur, G., Cozic, A., Caubel, A., Foujols, M., Meurdesoif, Y., Cadule, P., Devilliers, M., Ghattas, J., Lebas, N., Lurton, T., Mellul, L., Musat, I., Mignot, J., & Cheruy, F. (2018). IPSL IPSL-CM6A-LR model output prepared for CMIP6. Earth System Grid Federation. <https://doi.org/10.22033/ESGF/CMIP6.1534>
- Cantarelli, M. (2022). Circumscribing the host-range of *Aphthona nonstriata* Goeze (Coleoptera: Chrysomelidae), a candidate biocontrol agent for the invasive wetland plant *Iris pseudacorus* L. (Iridaceae). Vrije Universiteit Brussel [MSc Thesis].
- Cordeiro, P. F., Goulart, F. F., Macedo, D. R., Campos, M. D. C. S., & Castro, S. R. (2020). Modeling of the potential distribution of *Eichhornia crassipes* on a global scale: risks and threats to water ecosystems. *Revista Ambiente & Água*, 15. <https://doi.org/10.4136/ambi-agua.2421>
- De Jong, Y., Verbeek, M., Michelsen, V., de Place Bjørn, P., Los, W., Steeman, F., ... & Penev, L., 2014. Fauna Europaea – all European animal species on the web. *Biodiversity data journal*, (2), 10.3897/BDJ.2.e4034.

- Di Cola, V., Broennimann, O., Petitpierre, B., Breiner, F.T., d'Amen, M., Randin, C., Guisan, A., 2017. ecospat: an R package to support spatial analyses and modeling of species niches and distributions. *Ecography* 40 (6), 774–787. <https://doi.org/10.1111/ecog.02671>.
- Elith, J., Kearney, M., Phillips, S., 2010. The art of modelling range-shifting species. *Methods Ecol. Evol.* 1 (4), 330–342. <https://doi.org/10.1111/j.2041-210X.2010.00036.x>.
- Elith, J., Phillips, S.J., Hastie, T., Dudík, M., Chee, Y.E., Yates, C.J., 2011. A statistical explanation of MaxEnt for ecologists. *Divers. Distrib.* 17 (1), 43–57. <https://doi.org/10.1111/j.1472-4642.2010.00725.x>.
- Escobar, L. E., Lira-Noriega, A., Medina-Vogel, G., & Peterson, A. T. (2014). Potential for spread of the white-nose fungus (*Pseudogymnoascus destructans*) in the Americas: use of Maxent and NicheA to assure strict model transference. *Geospatial health*, 9(1), 221–229. <https://doi.org/10.4081/gh.2014.19>
- Essl, F., Lenzner, B., Bacher, S., Bailey, S., Capinha, C., Daehler, C., ... & Roura-Pascual, N. (2020). Drivers of future alien species impacts: An expert-based assessment. *Global Change Biology*, 26(9), 4880–4893. DOI: 10.1111/gcb.15199
- Fick, S.E., Hijmans, R.J., 2017. WorldClim 2: new 1km spatial resolution climate surfaces for global land areas. *Int. J. Climatol.* 37 (12), 4302–4315. <https://doi.org/10.1002/joc.5086>.
- Fielding, A.H., Bell, J.F., 1997. A review of methods for the assessment of prediction errors in conservation presence/absence models. *Environ. Conserv.* 24 (1), 38–49. <https://doi.org/10.1017/S0376892997000088>.
- GBIF (2020) GBIF Occurrence Download – *Iris pseudacorus*. <https://doi.org/10.15468/dl.b5y9hs>
- GBIF (2021) GBIF Occurrence Download – *Aphthona nonstriata*. <https://doi.org/10.15468/dl.uj5h6s>
- GBIF (2021) GBIF Occurrence Download – *Mononychus punctumalbum* <https://doi.org/10.15468/dl.zqdg6s>
- GBIF (2021) GBIF Occurrence Download – *Rhadinoceraea micans* <https://doi.org/10.15468/dl.uj5h6s>
- Gervazoni, P., Sosa, A., Franceschini, C., Coetzee, J., Fatthauser, A., Fuentes-Rodriguez, D., Martínez, A., Hill, M., 2020. The alien invasive yellow flag (*Iris pseudacorus* L.) in Argentinian wetlands: Assessing geographical distribution through different data sources. *Biol. Invasions* 22 (11), 3183–3193. <https://doi.org/10.1007/s10530-020-02331-4>.
- Gültekin, L., & Korotyaev, B. A. (2012). Ecological Description of Two Seed-Feeding Weevils of the Genus *Mononychus* Germar (Coleoptera: Curculionidae) on *Iris iberica* Hoffmann and *Iris spuria* L. in Northeastern Turkey. *The Coleopterists Bulletin*, 66(2), 155–161. <http://www.jstor.com/stable/23252999>
- Harms, N.E., Cronin, J.T., Diaz, R., Winston, R.L., 2020. A review of the causes and consequences of geographical variability in weed biological control successes. *Biol. Control* 151, 104398. <https://doi.org/10.1016/j.biocontrol.2020.104398>
- Harms, N.E., Knight, I.A., Pratt, P.D., Reddy, A.M., Mukherjee, A., Gong, P., Coetzee, J., Raghu, S., Diaz, R., 2021. Climate Mismatch Between Introduced Biological Control Agents and Their Invasive Host Plants: Improving Biological Control of Tropical Weeds in Temperate Regions. *Insects* 12 (6), 549. <https://doi.org/10.3390/insects12060549>
- Hijmans, R. J., 2017, raster: geographic analysis and modelling with raster data. R package version 2, 6-7, <https://CRAN.R-project.org/package=raster>.
- Hill, M.P. & Coetzee, J., 2017, 'The biological control of aquatic weeds in South Africa: Current status and future challenges', *Bothalia* 47(2), a2152. <https://doi.org/10.4102/abc.v47i2.2152>
- Hill, M. P., & Terblanche, J. S., 2014. Niche overlap of congeneric invaders supports a single-species hypothesis and provides insight into future invasion risk: implications for global management of the *Bactrocera dorsalis* complex. *PloS one*, 9(2), e90121. <https://doi.org/10.1371/journal.pone.0090121>.

- Hirzel, A.H., Le Lay, G., Helfer, V., Randin, C., Guisan, A., 2006. Evaluating the ability of habitat suitability models to predict species presences. *Ecol. Model.* 199 (2), 142–152. <https://doi.org/10.1016/j.ecolmodel.2006.05.017>.
- Hoelmer, K., and A. Kirk. 2005. Selecting arthropod biological control agents against arthropod pests: can the science be improved to decrease the risk of releasing ineffective agents? *Biological Control* 34:255–264. <https://doi.org/10.1016/j.biocontrol.2005.05.001>
- Hussner, A., Stiers, I., Verhofstad, M. J. J. M., Bakker, E. S., Grutters, B. M. C., Haury, J., ... & Hofstra, D. (2017). Management and control methods of invasive alien freshwater aquatic plants: a review. *Aquatic Botany*, 136, 112-137. <https://doi.org/10.1016/j.aquabot.2016.08.002>
- Jaca, T., Mkhize, V., 2015. Distribution of *Iris pseudacorus* (Linnaeus, 1753) in South Africa. *BioInvasions Records* 4 (4), 249–253. <https://doi.org/10.3391/bir.2015.4.4.03>.
- Kearney, M.R. & Porter W.P. (2009) Mechanistic niche modelling: combining physiological and spatial data to predict species' ranges. *Ecol Letters* 12, 334–350. <https://doi.org/10.1111/j.1461-0248.2008.01277.x>
- Kearney, M.R., Wintle, B.A., & Porter, W.P. (2010). Correlative and mechanistic models of species distribution provide congruent forecasts under climate change. *Conservation letters*, 3(3), 203-213. <https://doi.org/10.1111/j.1755-263X.2010.00097.x>
- Kriticos, D. J., Watt, M. S., Potter, K. J. B., Manning, L. K., Alexander, N. S., & Tallent-Halsell, N. (2011). Managing invasive weeds under climate change: considering the current and potential future distribution of *Buddleja davidii*. *Weed Research*, 51(1), 85-96. DOI: 10.1111/j.1365-3180.2010.00827.x
- Lobo, J.M., Jim ´enez-Valverde, A., Real, R., 2008. AUC: a misleading measure of the performance of predictive distribution models. *Glob. Ecol. Biogeogr.* 17 (2), 145–151. <https://doi.org/10.1111/j.1466-8238.2007.00358.x>.
- Manzoor, S.A., Griffiths, G., Lukac, M., 2018. Species distribution model transferability and model grain size–finer may not always be better. *Sci. Rep.* 8 (1), 1–9. <https://doi.org/10.1038/s41598-018-25437-1>.
- Martin, G.D., Magengelele, N.L., Paterson, I.D., Sutton, G.F., 2020. Climate modelling suggests a review of the legal status of Brazilian pepper *Schinus terebinthifolia* in South Africa is required. *S. Afr. J. Bot.* 132, 95–102. <https://doi.org/10.1016/j.sajb.2020.04.019>.
- McGrannachan, C., Barton, J., 2019. Feasibility of biological control of yellow flag iris, *Iris pseudacorus* L. (LC3487). *Manaaki Whenua - Landcare Res.* 63, pp.
- Merow, C., Smith, M.J., Silander Jr, J.A., 2013. A practical guide to MaxEnt for modeling species' distributions: what it does, and why inputs and settings matter. *Ecography* 36 (10), 1058–1069. <https://doi.org/10.1111/j.1600-0587.2013.07872.x>.
- Minuti, G., Coetzee, J.A., Ngxande-Koza, S., Hill, M.P., Stiers, I., 2021. Prospects for the biological control of *Iris pseudacorus* L. (Iridaceae). *Biocontrol Sci. Technol.* 31 (3), 314–335. <https://doi.org/10.1080/09583157.2020.1853050>.
- Minuti, G., Stiers, I., & Coetzee, J. A. (2022). Climatic suitability and compatibility of the invasive *Iris pseudacorus* L. (Iridaceae) in the Southern Hemisphere: Considerations for biocontrol. *Biological Control*, 169, 104886. <https://doi.org/10.1016/j.biocontrol.2022.104886>
- Mukherjee, A., Christman, M.C., Overholt, W.A., Cuda, J.P., 2011. Prioritizing areas in the native range of *hygrophila* for surveys to collect biological control agents. *Biol. Control* 56 (3), 254–262. <https://doi.org/10.1016/j.biocontrol.2010.11.006>.

- Mukherjee, A., Banerjee, A. K., & Raghu, S. (2021). Biological control of *Parkinsonia aculeata*: Using species distribution models to refine agent surveys and releases. *Biological Control*, 159, 104630. <https://doi.org/10.1016/j.biocontrol.2021.104630>
- Pearson, R.G., Raxworthy, C.J., Nakamura, M., Townsend Peterson, A., 2007. Predicting species distributions from small numbers of occurrence records: a test case using cryptic geckos in Madagascar. *J. Biogeogr.* 34 (1), 102–117. <https://doi.org/10.1111/j.1365-2699.2006.01594.x>.
- Pérez-De la O, N. B., Espinosa-Zaragoza, S., López-Martínez, V., D. Hight, S., & Varone, L. (2020). Ecological niche modeling to calculate ideal sites to introduce a natural enemy: The case of *Apanteles opuntiarum* (Hymenoptera: Braconidae) to control *Cactoblastis cactorum* (Lepidoptera: Pyralidae) in North America. *Insects*, 11(7), 454. <https://doi.org/10.3390/insects11070454>
- PESI 2022a. Maurizio Biondi. *Aphthona nonstriata* Goeze, 1777. Accessed through: Fauna Europaea at http://www.faunaeur.org/full_results.php?id=243304
- PESI 2022b. & Blank, Dr Stephan M. Taeger, Dr Andreas. *Rhadinoceraea* (Rhadinoceraea) *micans* (Klug, 1816). Accessed through: Fauna Europaea at http://www.faunaeur.org/full_results.php?id=355646
- Petitpierre, B., Broennimann, O., Kueffer, C., Daehler, C., & Guisan, A. (2017). Selecting predictors to maximize the transferability of species distribution models: Lessons from cross-continental plant invasions. *Global Ecology and Biogeography*, 26(3), 275–287. DOI: 10.1111/geb.12530
- Phillips, S.J., Anderson, R.P., Dudík, M., Schapire, R.E., Blair, M.E., 2017. Opening the black box: An open-source release of Maxent. *Ecography* 40 (7), 887–893. <https://doi.org/10.1111/ecog.03049>.
- Pyšek, P., Hulme, P. E., Simberloff, D., Bacher, S., Blackburn, T. M., Carlton, J. T., ... & Richardson, D. M. (2020). Scientists' warning on invasive alien species. *Biological Reviews*, 95(6), 1511–1534. doi: 10.1111/brv.12627
- QGIS Development Team, 2020. QGIS Geographic Information System. Open Source Geospatial Foundation Project, <http://qgis.osgeo.org>.
- R Development Core Team, 2019. R: A Language and Environment for Statistical Computing. Vienna, Austria: R Foundation for Statistical Computing.
- Riahi, K., Van Vuuren, D. P., Kriegler, E., Edmonds, J., O'Neill, B. C., Fujimori, S., ... & Tavoni, M. (2017). The shared socioeconomic pathways and their energy, land use, and greenhouse gas emissions implications: an overview. *Global environmental change*, 42, 153–168. <https://doi.org/10.1016/j.gloenvcha.2016.05.009>
- Ridley, J., Menary, M., Kuhlbrodt, T., Andrews, M., & Andrews, T. (2019). MOHC HadGEM3-GC31-LL model output prepared for CMIP6. Earth System Grid Federation. <https://doi.org/10.22033/ESGF/CMIP6.6109>
- Robertson, M.P., Kriticos, D.J., Zachariades, C., 2008. Climate matching techniques to narrow the search for biological control agents. *Biol. Control* 46 (3), 442–452. <https://doi.org/10.1016/j.biocontrol.2008.04.002>.
- Robinson, T.B., Martin, N., Loureiro, T.G., Matikinca, P., Robertson, M.P., 2020. Double trouble: the implications of climate change for biological invasions. *NeoBiota* 62, 463–487. <https://doi.org/10.3897/neobiota.62.55729>.
- Rodríguez-Merino, A., Fernández-Zamudio, R., García-Murillo, P., Muñoz, J., 2019. Climatic niche shift during *Azolla filiculoides* invasion and its potential distribution under future scenarios. *Plants* 8 (10), 424. <https://doi.org/10.3390/plants8100424>.
- Santamaría, L. (2002). Why are most aquatic plants widely distributed? Dispersal, clonal growth and small-scale heterogeneity in a stressful environment. *Acta oecologica*, 23(3), 137–154. [https://doi.org/10.1016/S1146-609X\(02\)01146-3](https://doi.org/10.1016/S1146-609X(02)01146-3)

- Schmitt, M., & Rbnn, T. (2011). Types of geographical distribution of leaf beetles (Chrysomelidae) in Central. *Research on Chrysomelidae* 3, 157, 131. <https://doi.org/10.3897/zookeys.157.1798>
- Shiogama, H., Abe, M., & Tatebe, H. (2019). MIROC MIROC6 model output prepared for CMIP6. Earth System Grid Federation. <https://doi.org/10.22033/ESGF/CMIP6.898>
- Sillero, N., Arenas-Castro, S., Enriquez-Urzelai, U., Vale, C. G., Sousa-Guedes, D., Martínez-Freiría, F., ... & Barbosa, A. M. (2021). Want to model a species niche? A step-by-step guideline on correlative ecological niche modelling. *Ecological Modelling*, 456, 109671. Simberloff, D. (2021). Maintenance management and eradication of established aquatic invaders. *Hydrobiologia*, 848(9), 2399-2420. <https://doi.org/10.1007/s10750-020-04352-5>
- Simberloff, D., Martin, J. L., Genovesi, P., Maris, V., Wardle, D. A., Aronson, J., ... & Vil`a, M., 2013. Impacts of biological invasions: what's what and the way forward. *Trends in ecology & evolution*, 28(1), 58-66. <https://doi.org/10.1016/j.tree.2012.07.013>
- Sun, Y., Brönnimann, O., Roderick, G.K., Poltavsky, A., Lommen, S.T., Müller-Sch`arer, H., 2017. Climatic suitability ranking of biological control candidates: a biogeographic approach for ragweed management in Europe. *Ecosphere* 8 (4), e01731. <https://doi.org/10.1002/ecs2.1731>.
- Sun, Y., Ding, J., Siemann, E., & Keller, S. R. (2020). Biocontrol of invasive weeds under climate change: progress, challenges and management implications. *Current opinion in insect science*, 38, 72-78. <https://doi.org/10.1016/j.cois.2020.02.003>
- Sutherland, W.J., 1990. Biological Flora of the British Isles: *Iris pseudacorus* L. *J. Ecol.* 78 (3), 833-848. <https://doi.org/10.2307/2260902>.
- Sutton, G.F., 2019. Searching for a needle in a haystack: where to survey for climatically-matched biological control agents for two grasses (*Sporobolus* spp.) invading Australia. *Biol. Control* 129, 37-44. <https://doi.org/10.1016/j.biocontrol.2018.11.012>.
- Trethowan, P. D., Robertson, M. P., & McConnachie, A. J., 2011. Ecological niche modelling of an invasive alien plant and its potential biological control agents. *South African Journal of Botany*, 77(1), 137-146, 10.1016/j.sajb.2010.07.007.
- USDA-APHIS 2013. Weed Risk Assessment for *Iris pseudacorus* L. (Iridaceae) – Yellow flag iris. USDA Animal and Plant Health Inspection Service, Version 1, 17pp. Available at: https://www.aphis.usda.gov/plant_health/plant_pest_info/weeds/downloads/wra/Iris_pseudacorus_WRA.pdf.
- Vignali, S., Barras, A. G., Arlettaz, R., & Braunisch, V. (2020). SDMtune: An R package to tune and evaluate species distribution models. *Ecology and Evolution*, 10(20), 11488-11506. <https://doi.org/10.1002/ece3.6786>
- Vilà, M., Basnou, C., Pyšek, P., Josefsson, M., Genovesi, P., Gollasch, S., ... & DAISIE partners. (2010). How well do we understand the impacts of alien species on ecosystem services? A pan-European, cross-taxa assessment. *Frontiers in Ecology and the Environment*, 8(3), 135-144. doi:10.1890/080083
- Zizka, A., Silvestro, D., Andermann, T., Azevedo, J., Duarte Ritter, C., Edler, D., Antonelli, A., 2019. CoordinateCleaner: Standardized cleaning of occurrence records from biological collection databases. *Methods Ecol. Evol.* 10 (5), 744-751. <https://doi.org/10.1111/2041-210X.13152>.

TABLES AND FIGURES

Table 1 – Details of the climatic suitability models computed in MaxEnt for *I. pseudacorus* and its candidate biocontrol agents. Each future model is named after the Global Circulation Model and Shared Socio-economic Pathway used as prediction (see section 2.1 for details). The total number of filtered occurrence records (#) is divided into training (70%) and testing (30%). Area under the receiving operator curve (AUC) are expressed as mean (\pm SD) of the 10 MaxEnt replicates computed for each model combination. AUC values close to 0.5 indicate a model no better than random, with values approaching 1 indicating perfect predictive performance (Fielding & Bell, 1997; but see Lobo et al., 2008 for a critique of this metric in presence-background modelling). As alternative evaluation metrics, the Continuous Boyce Index (CBI) and true presence ratio (TPR) are reported. CBI values range from -1 to 1, with positive values indicating model predictions consistent with the distribution of the presence data, values close to zero meaning that model predictions are no different from random, and negative values showing counter predictions (i.e. predicting no occurrence in areas where actual presence is recorded; Hirzel et al., 2006). The mean (\pm SD) 10th percentile omission rate (OR10) was used to estimate overfitting (values significantly different than the predicted 0.10 indicate an overfit model; Boria et al., 2014). The relative OR10 threshold was used to set the minimum suitability values to convert each model into binary predictions. The permutation importance of each predictor variable is reported for every model (variables with the highest contribution for each model are indicated in bold).

Sp	Model	# Records train/test	Test AUC (\pm SD)	CBI (\pm SD)	TPR (%)	OR10 train/test	OR10 Threshold	bio6	bio10	bio12	bio15	bio18
<i>I. pseudacorus</i>	Present climate	798/342	0.712 \pm 0.012	0.996 \pm 0.002	88.9	0.099/0.112	0.324	56.26	9.69	19.01	5.45	9.59
	HadGEM3_ssp24		0.723 \pm 0.012	0.996 \pm 0.003	89.8	0.098/0.099	0.323	52.07	8.91	28.84	3.72	6.47
	IPSL_ssp245		0.709 \pm 0.012	0.994 \pm 0.002	89.6	0.099/0.102	0.331	52.47	13.37	24.73	3.32	6.10
	MIROC6_ssp245		0.713 \pm 0.012	0.994 \pm 0.004	89.6	0.099/0.107	0.328	50.38	12.94	26.93	2.43	7.31
	HadGEM3_ssp58		0.719 \pm 0.012	0.995 \pm 0.002	89.2	0.098/0.110	0.314	51.17	14.29	20.98	2.86	10.70
	IPSL_ssp585		0.717 \pm 0.012	0.995 \pm 0.004	89.1	0.099/0.099	0.322	58.33	12.31	19.15	2.01	8.20
	MIROC6_ssp585		0.719 \pm 0.012	0.997 \pm 0.001	89.4	0.099/0.106	0.316	45.84	14.10	29.05	3.37	7.63
<i>A. nonstriata</i>	Present climate	234/100	0.898 \pm 0.010	0.983 \pm 0.007	88.4	0.097/0.116	0.249	58.47	24.02	3.10	9.05	5.37
	HadGEM3_ssp24		0.904 \pm 0.009	0.982 \pm 0.007	88.2	0.097/0.110	0.263	63.32	23.37	3.14	6.38	3.77
	IPSL_ssp245		0.905 \pm 0.010	0.989 \pm 0.005	89.0	0.097/0/106	0.262	58.73	22.15	3.21	13.07	2.85
	MIROC6_ssp245		0.896 \pm 0.010	0.984 \pm 0.006	88.5	0.097/0.114	0.262	59.55	21.81	3.34	10.08	5.22
	HadGEM3_ssp58		0.898 \pm 0.010	0.983 \pm 0.008	89.0	0.097/0.103	0.245	54.76	32.17	2.51	7.11	3.46
	IPSL_ssp585		0.901 \pm 0.010	0.986 \pm 0.003	89.3	0.097/0.112	0.272	57.86	21.61	2.48	14.01	4.03
	MIROC6_ssp585		0.900 \pm 0.010	0.984 \pm 0.007	89.7	0.098/0.102	0.261	61.27	22.44	2.25	9.09	4.96
<i>M. punctumalbum</i>	Present climate	220/94	0.875 \pm 0.014	0.980 \pm 0.009	89.8	0.097/0.105	0.196	44.65	35.20	5.46	14.70	-
	HadGEM3_ssp24		0.877 \pm 0.014	0.985 \pm 0.009	88.2	0.099/0.125	0.212	43.48	44.29	4.82	7.41	-
	IPSL_ssp245		0.882 \pm 0.013	0.983 \pm 0.007	91.5	0.099/0.084	0.210	41.47	44.73	3.23	10.58	-
	MIROC6_ssp245		0.877 \pm 0.014	0.982 \pm 0.014	88.6	0.098/0.114	0.204	44.29	37.57	2.61	15.54	-
	HadGEM3_ssp58		0.866 \pm 0.015	0.981 \pm 0.011	86.9	0.099/0.116	0.202	42.59	43.31	2.82	11.28	-
	IPSL_ssp585		0.883 \pm 0.013	0.986 \pm 0.006	90.7	0.099/0.086	0.203	42.03	41.87	2.33	13.76	-
	MIROC6_ssp585		0.878 \pm 0.014	0.985 \pm 0.005	88.6	0.098/0.110	0.198	42.56	40.32	6.69	10.43	-
<i>R. micans</i>	Present climate	126/54	0.956 \pm 0.009	0.946 \pm 0.022	88.7	0.094/0.111	0.214	78.86	9.82	3.45	1.21	6.67
	HadGEM3_ssp24		0.961 \pm 0.007	0.931 \pm 0.034	88.5	0.093/0.115	0.229	80.30	12.35	2.12	1.43	3.81
	IPSL_ssp245		0.960 \pm 0.008	0.935 \pm 0.051	88.7	0.091/0.100	0.222	77.96	14.08	3.27	0.16	4.54
	MIROC6_ssp245		0.957 \pm 0.008	0.943 \pm 0.027	88.7	0.091/0.111	0.217	77.94	11.73	4.79	0.57	4.97
	HadGEM3_ssp58		0.959 \pm 0.008	0.962 \pm 0.012	90.2	0.090/0.104	0.236	77.71	9.47	6.31	0.61	5.89
	IPSL_ssp585		0.958 \pm 0.008	0.994 \pm 0.034	85.7	0.091/0.133	0.256	79.14	10.78	4.40	0.70	4.99
	MIROC6_ssp585		0.961 \pm 0.007	0.952 \pm 0.028	87.2	0.092/0.119	0.248	83.38	7.81	2.78	0.28	5.75

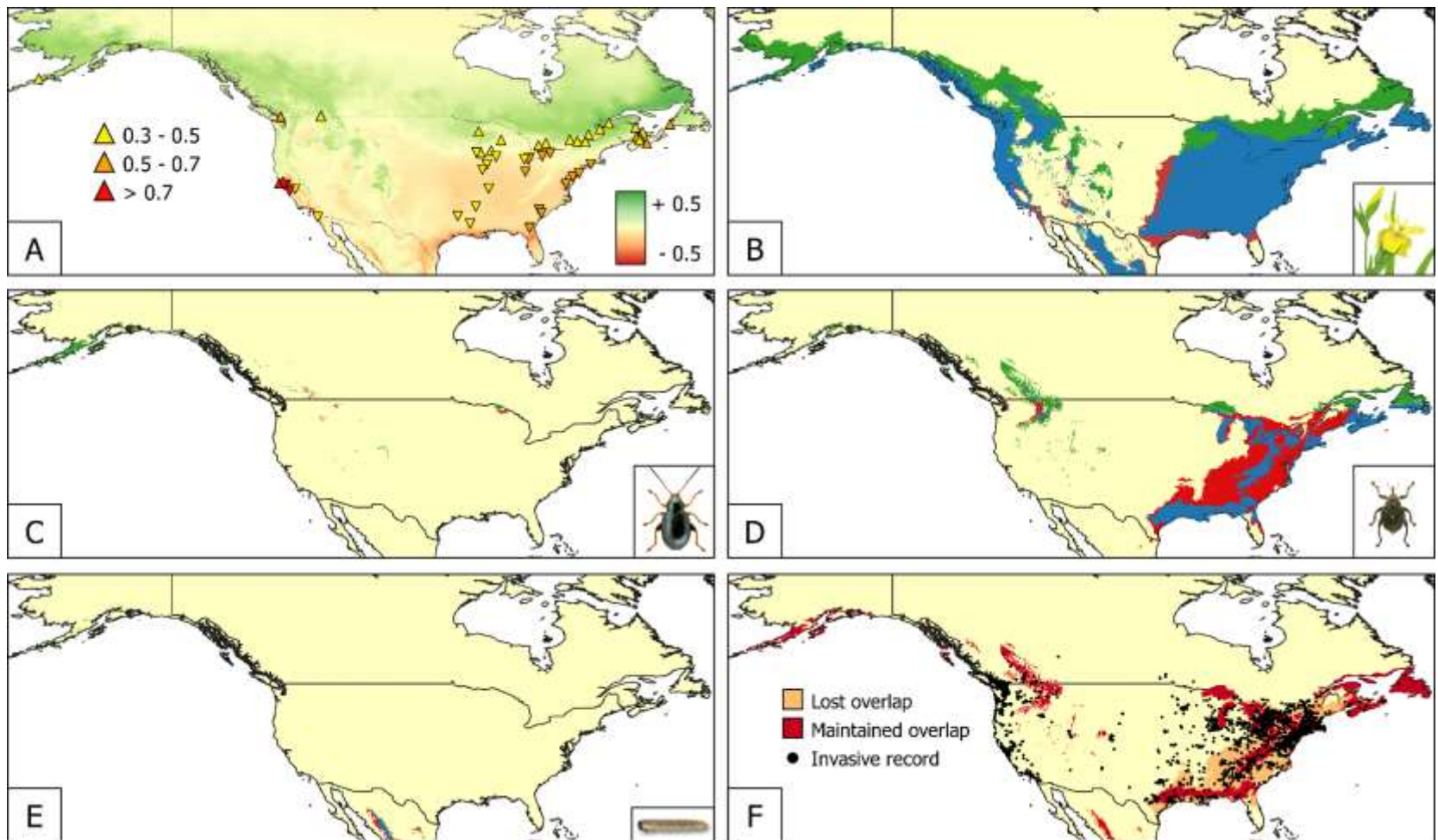


Figure 1 – Invasion risk, climatic suitability and biocontrol potential for *Iris pseudacorus* in North America. **(A)** Net change in suitability for *I. pseudacorus* between present and future climatic conditions (green indicates an increase in suitability, red a decrease). Ramsar sites at risk of invasion are represented by triangles: colours represent their current suitability score; upward and downward direction indicate if suitability is predicted to increase or decrease in the future. Binary suitability maps for **(B)** *I. pseudacorus*, **(C)** *Aphthona nonstriata*, **(D)** *Mononychus punctumalbum*, and **(E)** *Rhadinoceraea micans* show areas where suitability will be gained (green), lost (red), or maintained (blue) under future climatic conditions. **(F)** Climatic niche overlap between *I. pseudacorus* and its candidate biocontrol agents based on present and predicted future climatic conditions. Black dots indicate present occurrence records of the weed.

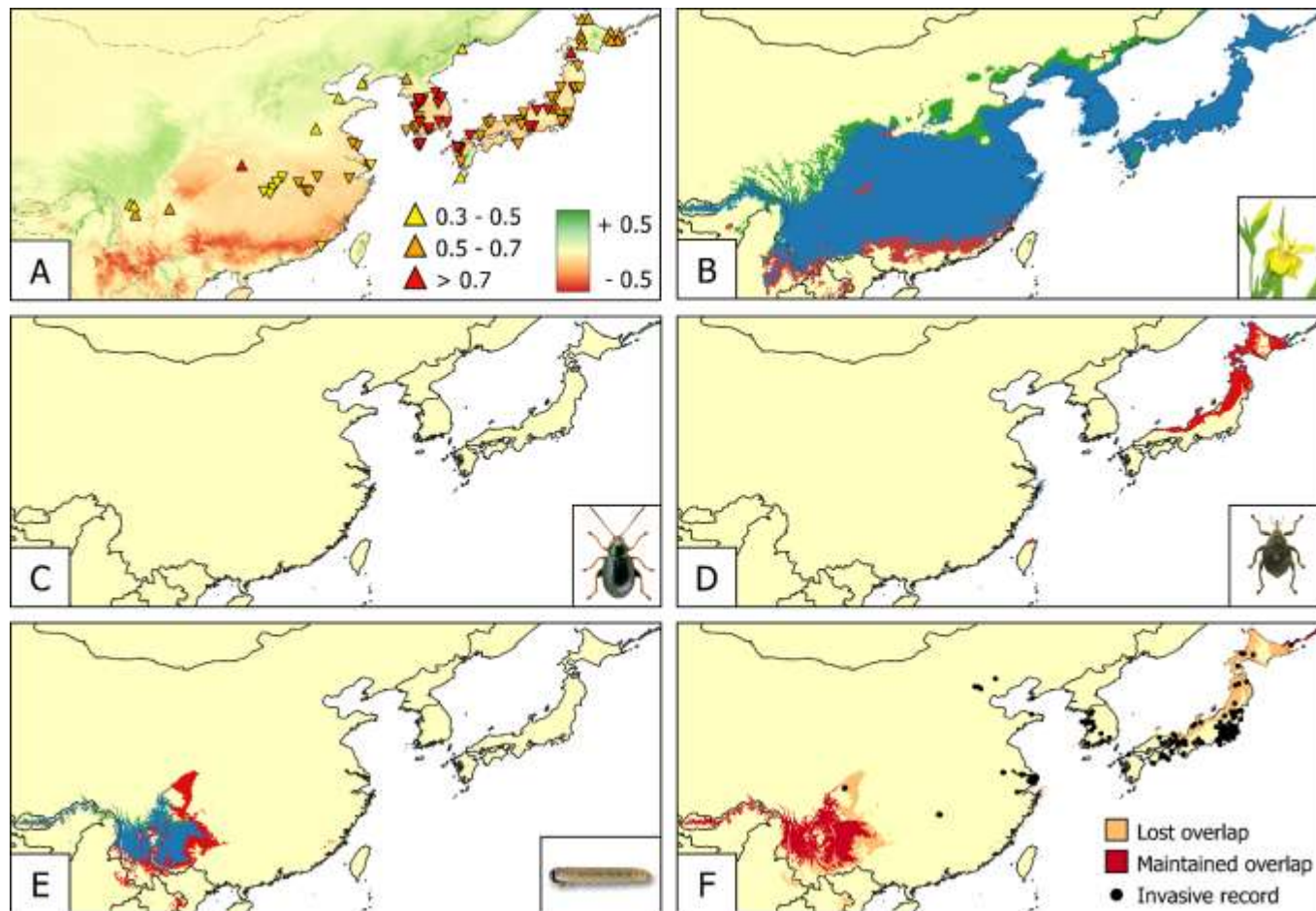


Figure 2 - Invasion risk, climatic suitability and biocontrol potential for *Iris pseudacorus* in Eastern Asia. **(A)** Net change in suitability for *I. pseudacorus* between present and future climatic conditions (green indicates an increase in suitability, red a decrease). Ramsar sites at risk of invasion are represented by triangles: colours represent their current suitability score; upward and downward direction indicate if suitability is predicted to increase or decrease in the future. Binary suitability maps for **(B)** *I. pseudacorus*, **(C)** *Aphthona nonstriata*, **(D)** *Mononychus punctumalbum*, and **(E)** *Rhadinoceraea micans* show areas where suitability will be gained (green), lost (red), or maintained (blue) under future climatic conditions. **(F)** Climatic niche overlap between *I. pseudacorus* and its candidate biocontrol agents based on present and predicted future climatic conditions. Black dots indicate present occurrence records of the weed.

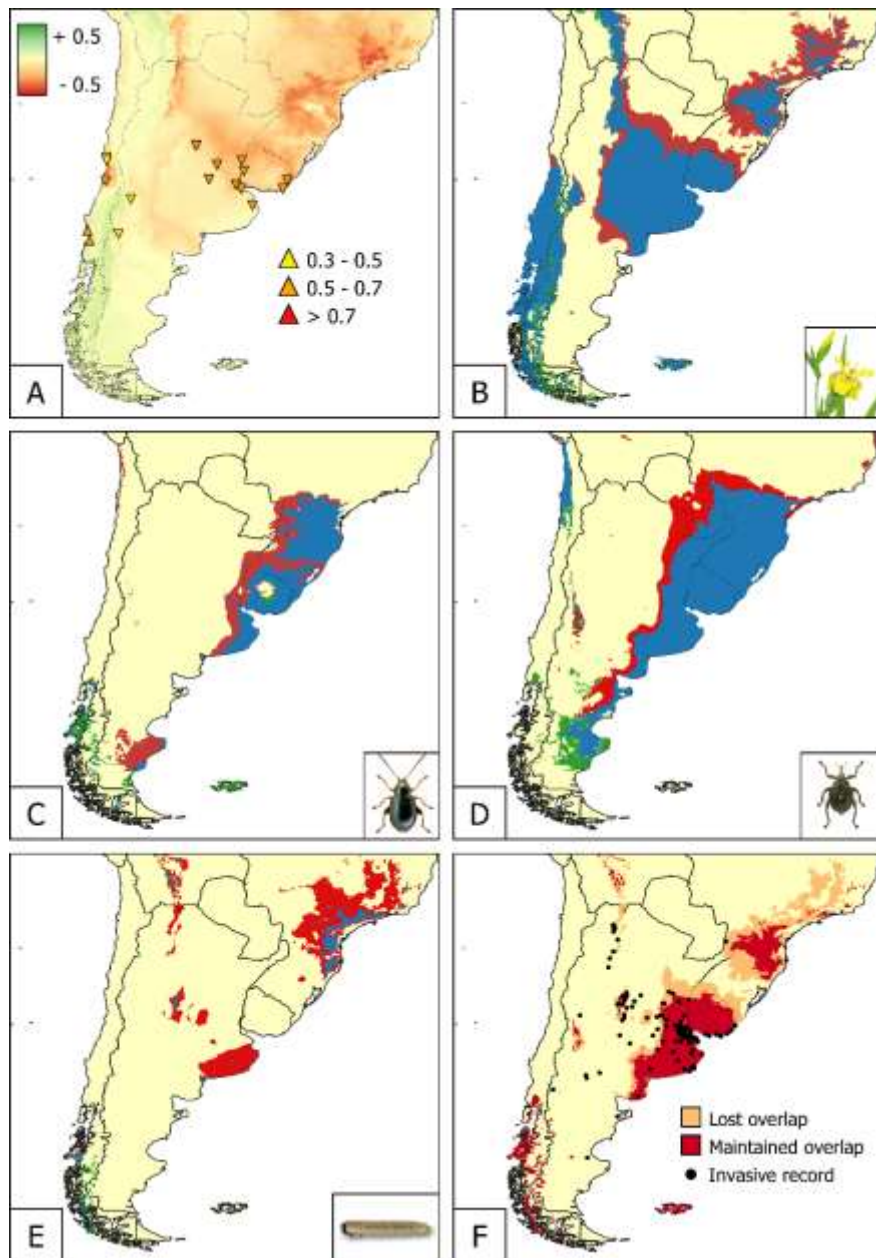


Figure 3 - Invasion risk, climatic suitability and biocontrol potential for *Iris pseudacorus* in South America. **(A)** Net change in suitability for *I. pseudacorus* between present and future climatic conditions (green indicates an increase in suitability, red a decrease). Ramsar sites at risk of invasion are represented by triangles: colours represent their current suitability score; upward and downward direction indicate if suitability is predicted to increase or decrease in the future. Binary suitability maps for **(B)** *I. pseudacorus*, **(C)** *Aphthona nonstriata*, **(D)** *Mononychus punctumalbum*, and **(E)** *Rhadinoceraea micans* show areas where suitability will be gained (green), lost (red), or maintained (blue) under future climatic conditions. **(F)** Climatic niche overlap between *I. pseudacorus* and its candidate biocontrol agents based on present and predicted future climatic conditions. Black dots indicate present occurrence records of the weed.

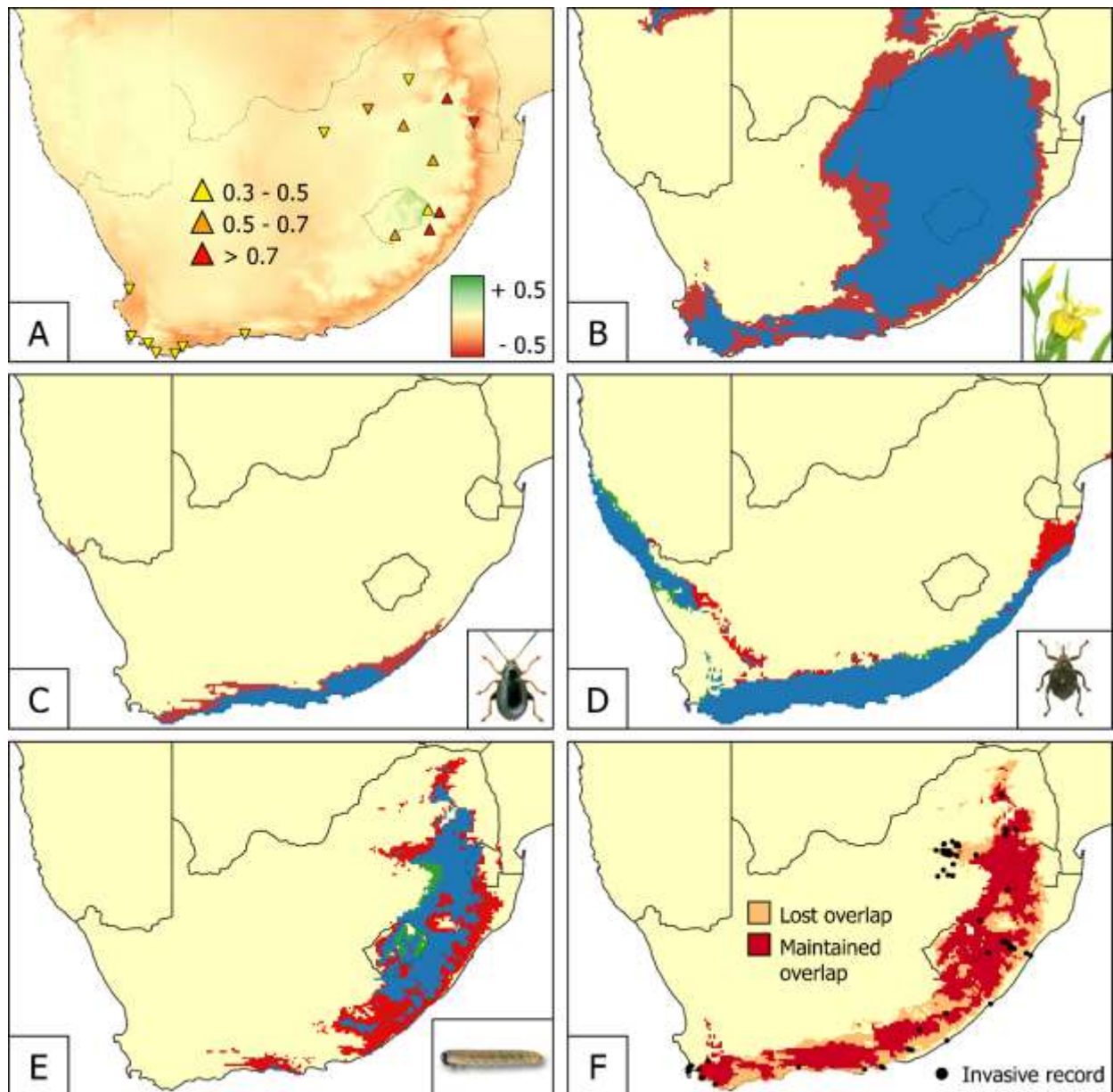


Figure 4 - Invasion risk, climatic suitability and biocontrol potential for *Iris pseudacorus* in South Africa. **(A)** Net change in suitability for *I. pseudacorus* between present and future climatic conditions (green indicates an increase in suitability, red a decrease). Ramsar sites at risk of invasion are represented by triangles: colours represent their current suitability score; upward and downward direction indicate if suitability is predicted to increase or decrease in the future. Binary suitability maps for **(B)** *I. pseudacorus*, **(C)** *Aphthona nonstriata*, **(D)** *Mononychus punctumalbum*, and **(E)** *Rhadinoceraea micans* show areas where suitability will be gained (green), lost (red), or maintained (blue) under future climatic conditions. **(F)** Climatic niche overlap between *I. pseudacorus* and its candidate biocontrol agents based on present and predicted future climatic conditions. Black dots indicate present occurrence records of the weed.

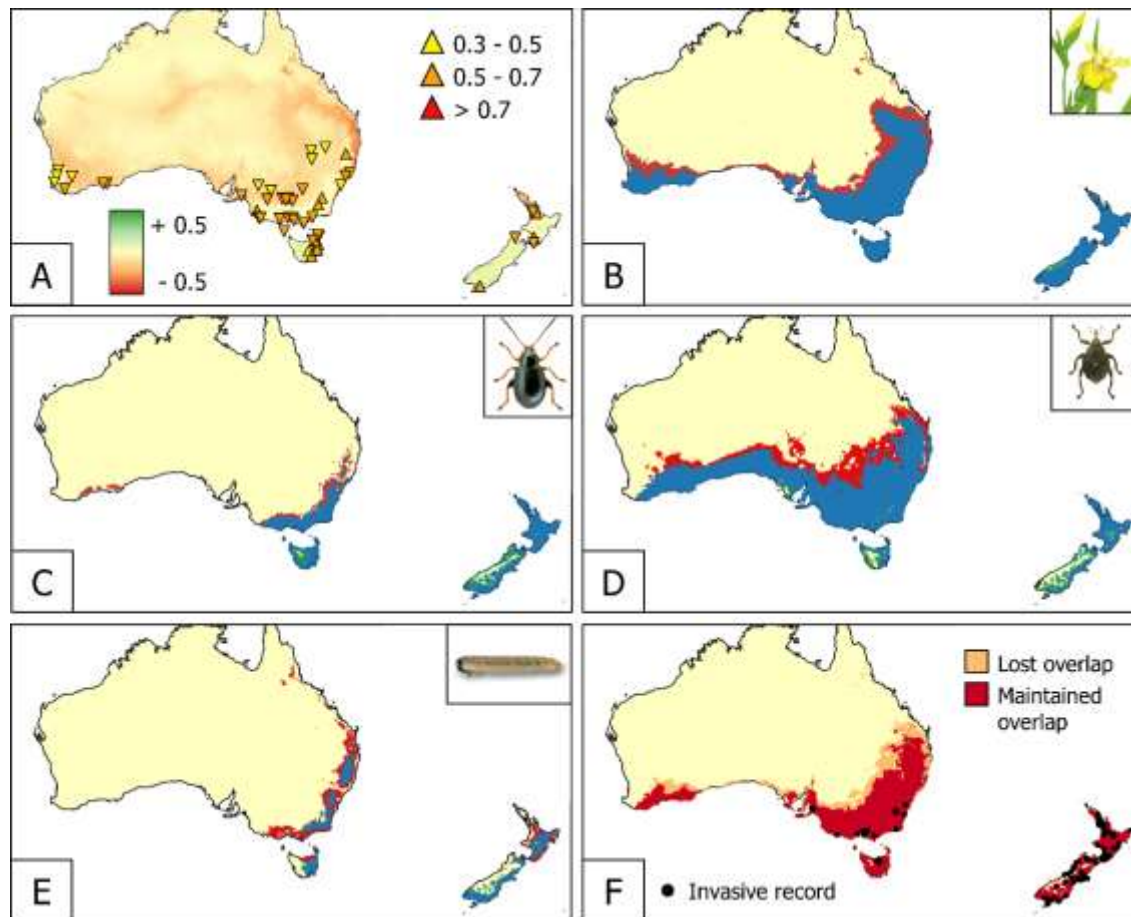
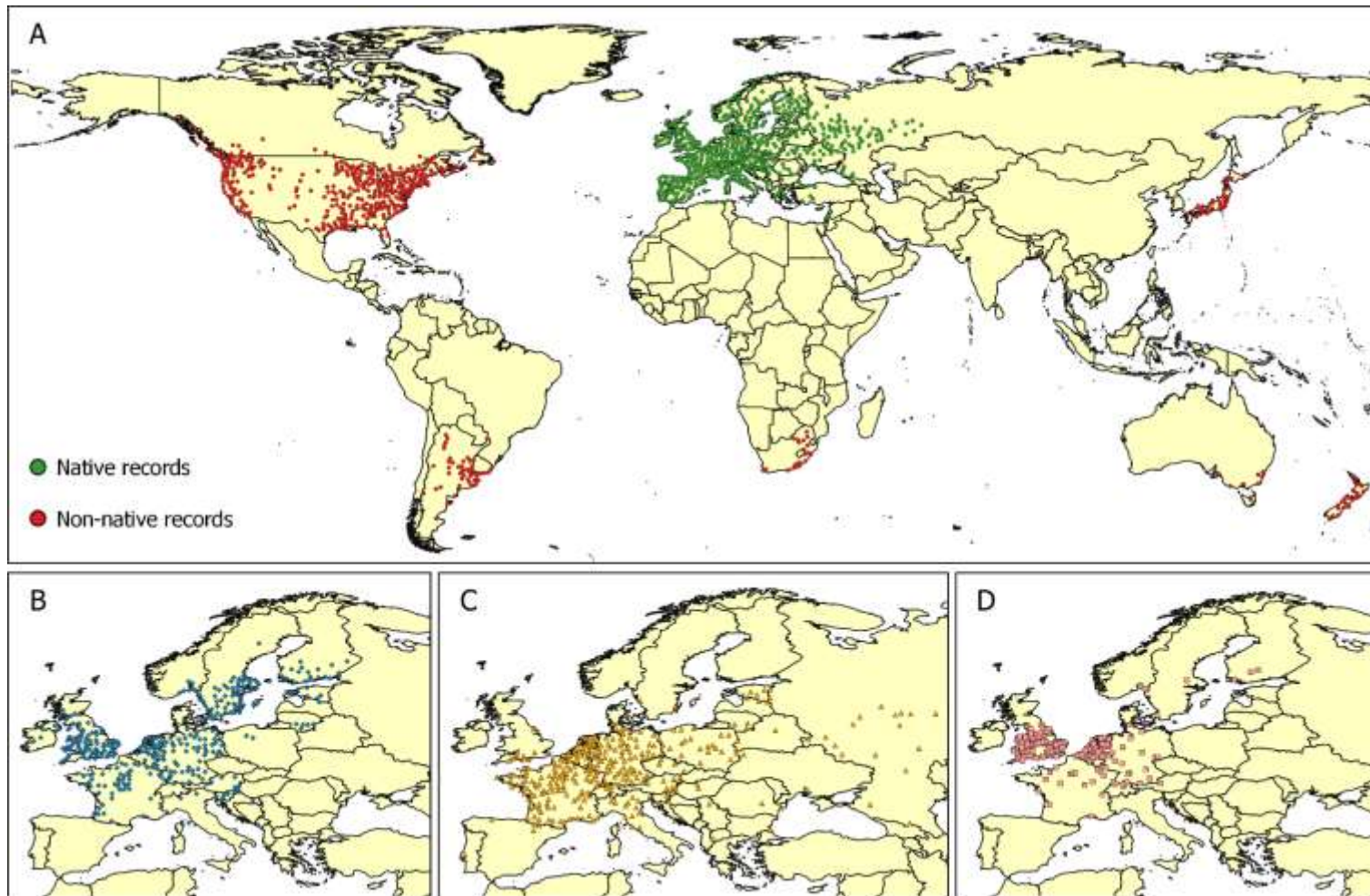
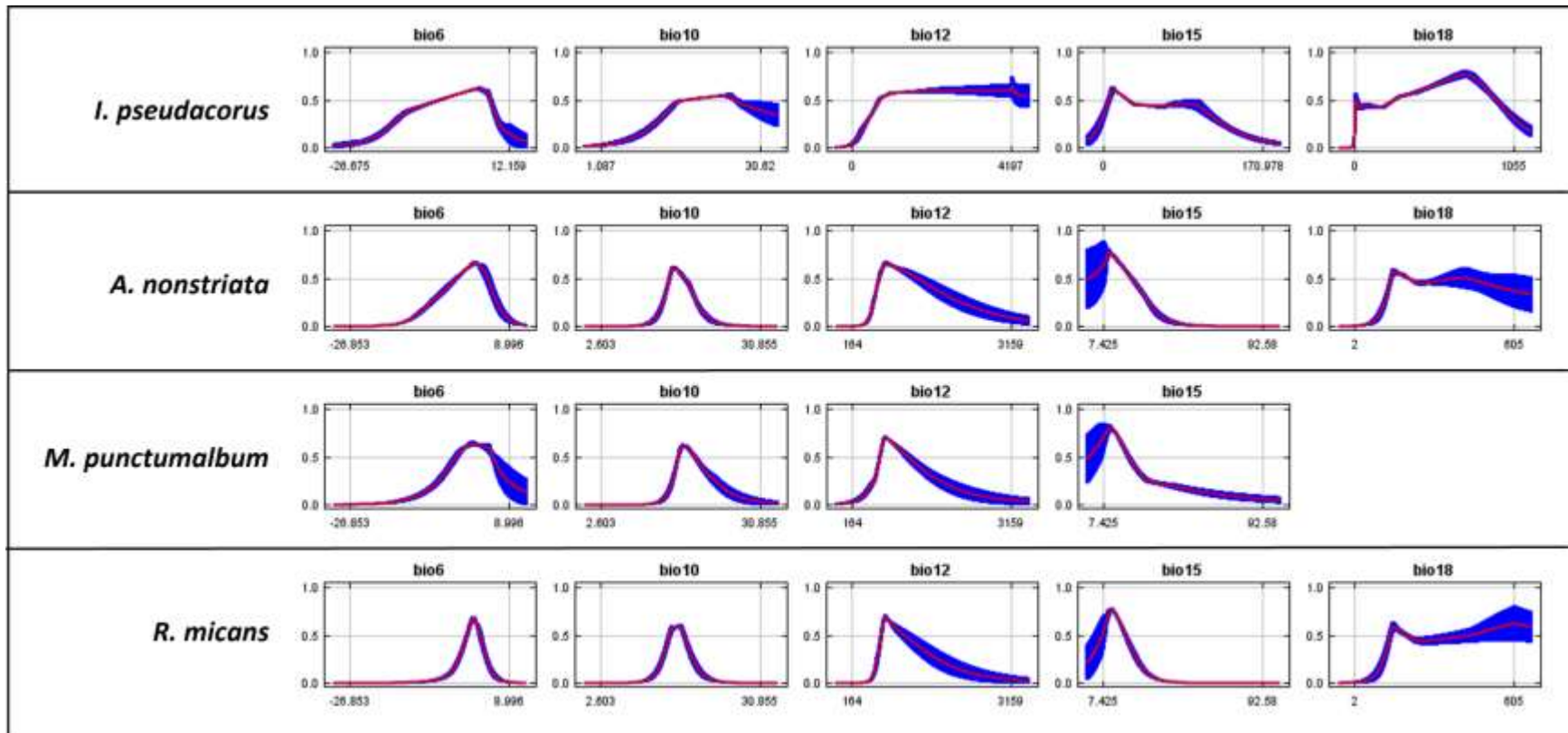


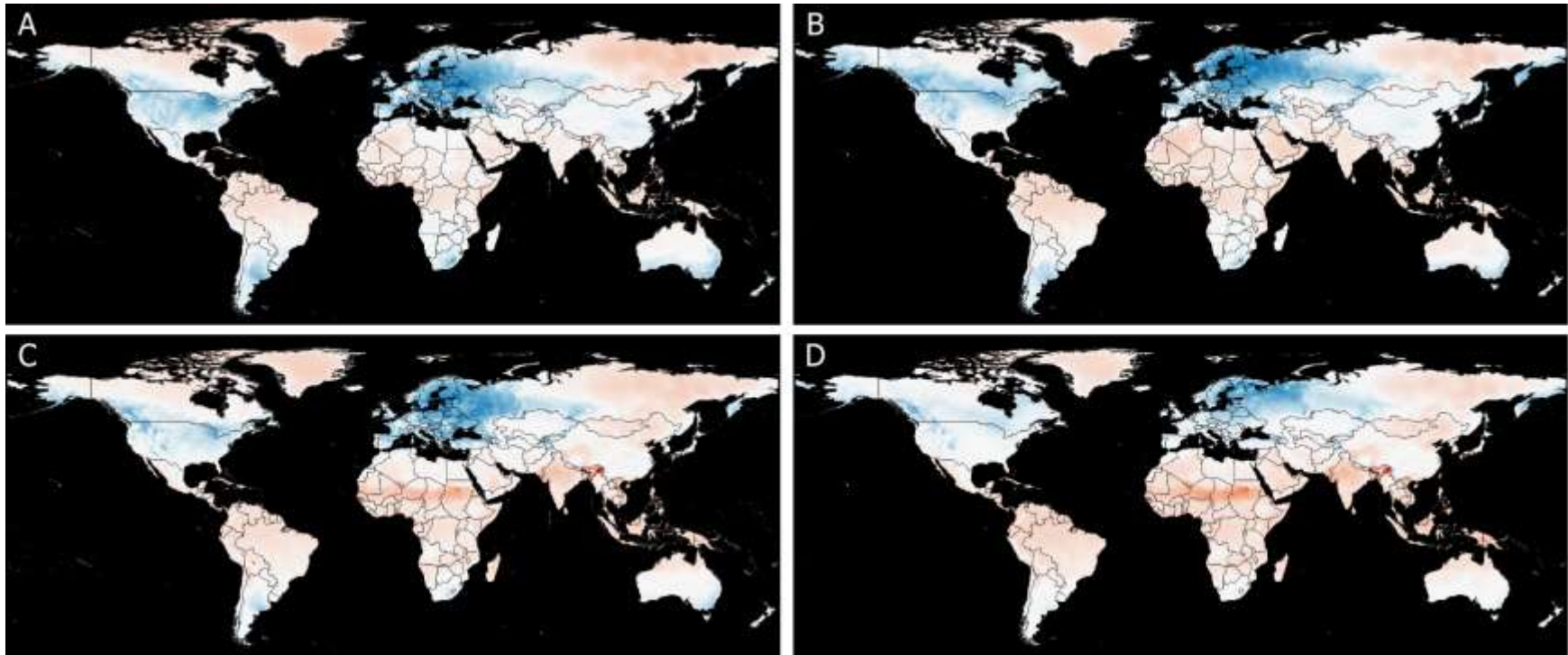
Figure 5 - Invasion risk, climatic suitability and biocontrol potential for *Iris pseudacorus* in Australasia. **(A)** Net change in suitability for *I. pseudacorus* between present and future climatic conditions (green indicates an increase in suitability, red a decrease). Ramsar sites at risk of invasion are represented by triangles: colours represent their current suitability score; upward and downward direction indicate if suitability is predicted to increase or decrease in the future. Binary suitability maps for **(B)** *I. pseudacorus*, **(C)** *Aphthona nonstriata*, **(D)** *Mononychus punctumalbum*, and **(E)** *Rhadinoceraea micans* show areas where suitability will be gained (green), lost (red), or maintained (blue) under future climatic conditions. **(F)** Climatic niche overlap between *I. pseudacorus* and its candidate biocontrol agents based on present and predicted future climatic conditions. Black dots indicate present occurrence records of the weed.



Supplementary Figure S1 – Occurrence records (after data cleaning and filtering) used for modelling their present and future climate suitability of **A)** *Iris pseudacorus*; **B)** *Aphthona nonstriata*; **C)** *Mononychus punctumalbum*; and **D)** *Rhadinoceraea micans* (see GBIF 2020, 2021 for original datasets).



Supplementary Figure S2 – Response curves of the climatic suitability models computed during the study. The curves show how the predicted climatic suitability (Y axis) changes in response to the variation of each environmental variable (X axis), independently of the other variables. The curves show the mean response (red) and the standard deviation (blue) of 10 replicate Maxent runs (Phillips et al., 2017).



Supplementary Figure S3 - Multivariate Environmental Similarity Surface (MESS) between the range of variables used for training the climatic suitability models and the range encountered in the projection layers. Areas having one or more environmental variables outside the range present in the training data are shown in red, so predictions in those areas should be treated with caution. **A)** Model for *I. pseudacorus*, projected on current climate; **B)** Model for *I. pseudacorus*, projected on future climate; **C)** Model for the biocontrol agents, projected on current climate; **D)** Model for the biocontrol agents, projected on future climate. Note that the regions of interest for our study show high environmental similarity with the training data (blue to white colour), indicating reliable model transferability (see Elith et al., 2010 for details).